The Existence of Inner Cool Disks in the Low Hard State of Accreting Black Holes

B. F. Liu

National Astronomical Observatories/Yunnan Observatory, Chinese Academy of Sciences, P.O. Box 110, Kunming 650011, China

bfliu@ynao.ac.cn

Ronald E. Taam

Northwestern University, Department of Physics and Astronomy, 2131 Tech Drive, Evanston, IL 60208; ASIAA/National Tsing Hua University - TIARA, Hsinchu, Taiwan

r-taam@northwestern.edu

E. Meyer-Hofmeister

Max-Planck-Institut für Astrophysik, Karl Schwarzschildstr. 1, D-85740, Garching, Germany

emm@mpa-garching.mpg.de

and

F. Meyer

Max-Planck-Institut für Astrophysik, Karl Schwarzschildstr. 1, D-85740, Garching, Germany

frm@mpa-garching.mpg.de

ABSTRACT

The condensation of matter from a corona to a cool, optically thick inner disk is investigated for black hole X-ray transient systems in the low hard state. A description of a simple model for the exchange of energy and mass between corona and disk originating from thermal conduction is presented, taking into account the effect of Compton cooling of the corona by photons from the underlying disk. It is found that a weak, condensation-fed inner disk can be present in the low hard state of black hole transient systems for a range of luminosities which

depend on the magnitude of the viscosity parameter. For $\alpha \sim 0.1 - 0.4$ an inner disk can exist for luminosities in the range $\sim 0.001 - 0.02 L_{Edd}$. The model is applied to the X-ray observations of the black hole candidate sources GX 339-4 and Swift J1753.5-0127 in their low hard state. It is found that Compton cooling is important in the condensation process, leading to the maintenance of cool inner disks in both systems. As the results of the evaporation/condensation model are independent of the black hole mass, it is suggested that such inner cool disks may contribute to the optical and ultraviolet emission of low luminosity active galactic nuclei.

Subject headings: accretion, accretion disks — black hole physics — X-rays: stars — X-rays: binaries — stars:individual (GX 339-4, Swift J1753.5-0127)

1. Introduction

Black hole X-ray transient binary systems have attracted increasing attention in recent years since they can be used as a probe of the underlying physics of the accretion process in disks surrounding black holes over a wide range in luminosity. The X-ray spectral behavior of these systems is complex, exhibiting differing states and transitions. In particular, it is well known that two basic X-ray spectral states are present with a soft spectral state occurring at high luminosities and a hard spectral state occurring at low luminosities. The properties of these systems have been reviewed by Tanaka & Shibazaki (1996) and more recently by Remillard & McClintock (2006) and McClintock & Remillard (2006). It is now generally accepted that these two spectral states originate from different accretion modes dependent on the mass accretion rate.

At high luminosities, black hole X-ray transients are characterized by a soft thermal spectrum described by a multi-color black body component dominant at about 1 keV. This has been interpreted as arising from an optically thick accretion disk extending to the innermost stable circular orbit (Shakura & Sunyaev 1973). In contrast, at low luminosities, the systems are characterized by a hard spectral state where the spectrum is described by a power law with a typical photon index of about 1.7. The emission is commonly thought to be produced by the Compton scattering of soft photons with the hot electrons in an optically thin inner disk (Shapiro et al. 1976; Sunyaev & Titarchuk 1980; Pozdnyaknov et al. 1983). In these models, the ions and electrons are described by a two temperature plasma. Here, the ions are heated to high temperatures by viscous dissipation, the electrons to attain lower temperatures due to their strong interaction with radiation and weak Coulomb coupling with ions. The initial models developed for this state (Shapiro et al. 1976) were thermally

unstable, and it has been recognized that the radial advection of internal energy can stabilize the flow (see, for example, Narayan 2005). In this case, the internal energy is advected inward with the flow, resulting in an inefficient conversion of gravitational potential energy to radiation (e.g., Narayan & Yi 1994; Narayan & Yi 1995a,b). The radius of transition between the cool outer disk and the hot advection-dominated inner disk was not theoretically determined, but obtained by fits to the observational data (see Esin et al. 1997).

The transition between these states occurs at luminosities in the range of $\sim 1 - 4\%$ of the Eddington value (Maccarone 2003) and is thought to be a consequence of a disk corona interaction (Meyer, Liu, & Meyer-Hofmeister 2000b). More detailed observations and analyses indicated that, in addition to the soft and hard state, an intermediate state could occur during the rise or decay of an outburst between the hard and soft state. Here, both a soft thermal spectrum and a hard power law spectrum are observed, likely indicating the coexistence of a hot optically thin and cool optically thick disk structure. Such a disk structure can be envisaged if the optically thick disk is truncated by some evaporative process, leading to the formation of an inner hot geometrically thick, optically thin disk surrounded by an outer cool geometrically thin disk. Originally, the idea of a two phase accretion structure was suggested by Eardley et al. (1975) and Shapiro et al. (1976). Such disk geometries have recently been calculated based on a proton bombardment model (Dullemond & Spruit 2005) and a coronal evaporation model controlled by electron conduction (Liu et al. 1999, Różańska & Czerny 2000a,b). In the latter case a maximum evaporation rate was found which allowed an estimate of a smallest transition radius and a maximal mass flow rate for which the evaporation rate into the corona can still exceed the mass flow rate in the cool outer disk (Liu et al. 1999). Alternatively Liu, Meyer, & Meyer-Hofmeister (2006) and Meyer, Liu, & Meyer-Hofmeister (2007) have suggested that a remnant cool inner disk formed during the thermally dominant (soft) spectral state, when the accretion rate declines just below the transition rate, can be maintained for times longer than a viscous diffusion time by condensation of matter from the corona. The accretion geometry then would be described as a cool inner and even cooler outer disk separated by a gap filled with an advection dominated accretion flow (ADAF) (Fig. 1, see also Mayer & Pringle 2007). Here, the inner cool disk is responsible for the presence of the soft thermal component coexisting with the hard component formed in the coronal region.

Recently, evidence pointing to the possible presence of a cool inner disk during the low hard state of black hole transient systems has been provided by observations of GX 339-4 and Swift J1753.5-0127 (Miller et al. 2006a,b). In particular, Miller et al. (2006a) find that a soft thermal component ($kT \sim 0.2$ keV) is required to fit the spectrum of J1753.5-0127, with a normalization suggesting a small inner disk region. Similarly, a soft thermal component characterized by kT $\sim$ 0.3 keV was required for GX 339-4 (Miller et al. 2006b). In this

latter case, a broad Fe K line was also required to fit the spectrum, providing additional evidence to support the hypothesis of cold matter lying close to the black hole. We note that this interpretation is model dependent since it is possible that the emission line may have formed in an outflowing wind (Laurent & Titarchuk 2007). Nevertheless, the existence of such an inner cold disk region is very suggestive. Such a picture may be consistent with the accretion geometry envisaged by Liu et al. (2006) and Meyer et al. (2007), or cold clumps in luminous hot accretion flows (Yuan 2003). However, Miller et al. (2006b) find evidence for a soft component from a weak disk extending to the innermost stable circular orbit (ISCO) at X-ray luminosities as low as 0.003 L_{Edd}, significantly less than the luminosity corresponding to the transition between the high soft and low hard states.

In this paper, we investigate the properties of a cool inner disk within the framework of the coronal evaporation and recondensation model, extending earlier work by Liu et al. (2006) and Meyer et al. (2007), to determine whether cool disks are present at low X-ray luminosities. In contrast to Liu et al. (2006) and Meyer et al. (2007), we include the cooling effect associated with the inverse Compton scattering of photons emitted by an underlying disk on hot thermal electrons for determining the thermal state of the corona. Assuming that thermal conduction determines the energy and mass exchange between corona and underlying cool disk, we examine the range of conditions under which a cool inner disk forms and is maintained. In the next section we give an overview of the evaporation/condensation model, including the additional input physics. In §3 illustrative results are presented for the case where the cooling of electrons is dominated by heat conduction to the underlying disk and for the case where electron cooling is dominated by Compton scattering of cool photons. To illustrate the potential applicability of these concepts to observed sources, we compare the numerical results to the X-ray observations of the black hole candidate source GX 339-4 and the recently discovered system Swift J1753.5-0127 (Palmer et al. 2005) in §4. Finally, we discuss our results and their implications in the last section.

2. Theoretical Model

The formation of a corona above a geometrically thin disk may result from physical processes similar to those operating in the solar corona or from a thermal instability (e.g., Shaviv & Wehrse 1986) in the uppermost layers of a disk. As mentioned above, earlier work (Meyer & Meyer-Hofmeister 1994; Meyer, Liu, & Meyer-Hofmeister 200a, Liu et al. 2002; Ròżańska & Czerny 2000a,b) revealed that a disk corona fed by the evaporation of matter from an underlying cool disk can be maintained as an accreting coronal flow. The description of the mechanism responsible for the evaporation is briefly described below.

In the corona, the viscous dissipation leads to ion heating, which is partially transferred to the electrons via Coulomb collisions. This energy is assumed to be conducted into a lower, cooler transition layer. If the density in this layer is sufficiently high, the conductive flux is radiated away. On the other hand, if the density is insufficient to efficiently radiate the energy, the underlying cool gas is heated and evaporation into the corona takes place. The evaporated matter carries angular momentum, and it gradually accretes onto the central black hole as a result of viscous transport. As the accreted gas is resupplied by the material evaporated from the cool disk, a steady accreting corona is formed above the disk in which a balance of evaporation and accretion is achieved.

While the disk evaporation provides matter for accretion in the corona, the mass accretion through the cool outer disk is decreased and can even vanish at distances where the inflowing rate is lower than the evaporation rate, approximated by $\dot{M}_{\rm evap} \equiv 4\pi R^2 \dot{m}_0$, where $\dot{m}_0$ is the evaporation rate per unit area from the disk into the corona. Numerical calculations (Meyer et al. 2000a; Liu et al. 2002) reveal that the evaporation rate increases with decreasing distance to the central object until a maximum evaporation rate of about a percent of the Eddington rate is reached at a distance of several hundred Schwarzschild radii. The existence of such a maximum leads to a change in character of the accretion geometry. If the mass flow in the disk is below this maximum value, as in the quiescent state of black hole X-ray transients, the optically thick disk is truncated at the distance where all matter is evaporated, leaving a pure advection dominated coronal flow. As the mass flow rate increases (e.g., during the rise to an outburst), the edge of the cool optically thick disk moves inward. If the mass flow in the disk increases above the maximal evaporation rate, the disk can not be evaporated completely and, hence, the cool disk extends to the ISCO. During the decline from the peak of the outburst, the inner edge of the cool disk retreats outwards to greater distances from the central black hole. These variations in the accretion process during the outburst of a black hole X-ray transient system provide explanation for the hard and soft states in these systems (Meyer et al. 2000b). Recent investigations (Liu et al. 2006; Meyer et al. 2007) furthermore reveal that when the accretion rate is not far below the maximal evaporation rate an inner disk separated from the outer disk by a coronal region could also exist, leading to an intermediate state of black hole accretion.

The onset of an intermediate state occurs as the accretion rate decreases just below the maximal evaporation rate. At this time, disk truncation by evaporation sets in near the region where the evaporation rate is maximal. A coronal gap appears and widens with a further decrease in the accretion rate with the inner cool disk reduced in extent. Because of diffusion, the inner disk can not survive for a time longer than a viscous time (which is only a few days in the inner disk) unless matter continuously condenses from the ADAF onto the cool inner disk. In the following we investigate the interaction between the disk and the

corona/ADAF, showing the conditions under which matter condenses onto the inner disk, thereby maintaining a cool disk in the inner region.

2.1. Model Assumptions

The corona lying above an inner cool disk is similar to an ADAF. The main physical differences between these two descriptions stem from the existence of vertical thermal conduction caused by the large temperature gradient between the corona and the disk and the presence of cool disk photons, which upon propagating through the corona remove energy by inverse Compton scattering. At low accretion rates, neither conduction nor Compton scattering is important for energy loss and the corona is described by an ADAF. In this study, we assume that the corona above the cool disk can be described by an ADAF, where the structure (such as pressure, density, and ion temperature) is determined by the mass of the black hole, the mass accretion rate, and the viscosity at a given distance (Narayan & Yi 1995a). However, the cooling in such an ADAF is assumed to be either dominated by the Compton scattering of the disk photons or dominated by vertical heat conduction. That is, we implicitly assume that non-thermal (e.g., synchrotron) processes are unimportant in the lowest level of approximation. As we shall see, such a simple model contains the ingredients necessary to provide an understanding of the soft spectrum in the low/hard state. The model allows an analytical description, revealing the dependence of the disk size, effective temperature, luminosity, and spectrum on the black hole mass, mass accretion rate, and disk viscosity.

2.2. Conductive Cooling-Dominant Corona

The condensation from a corona where cooling results mainly from conduction has been studied in earlier works by Liu et al. (2006) and Meyer et al. (2007). We introduce the main results here for completeness and for comparison to the case where the cooling by the inverse Compton scattering process is dominant (see §2.3). In the bulk of the corona the thermal state of the ions is not significantly affected by conductive cooling of the electrons until the electron temperature has become low enough near the base of the corona so that collisional coupling between the ions and electrons becomes effective. From this coupling interface down to the upper layers of the cool disk the ion temperature, T_i, and electron temperature, T_e, no longer differ. This results in a dramatic decline of T_i, leading to a significant increase in density as the pressure in the vertical extent changes little in comparison to the change in temperature. As a consequence, bremsstrahlung energy losses become much

more important in this layer than in a typical ADAF. Henceforth, this layer is referred to as the radiating layer. The pressure in the ADAF is of particular interest since it determines whether evaporation or condensation takes place. For example, at sufficiently high pressure, bremsstrahlung can be so efficient that not only is all the heat drained from the ADAF by thermal conduction radiated away, but also the gas in the radiating layer is further cooled, leading to condensation onto the disk. On the other hand, if the pressure in the upper corona is sufficiently low so that the density in the radiating layer is too low to radiate away the conductive flux, disk matter is evaporated into the corona. We adopt for our analysis the values derived by Narayan & Yi (1995b). The ADAF pressure, density, viscous heating rate, and sound speed depend on the viscosity parameter, α, black hole mass, m, the accretion rate, $\dot{m}$, and r the distance from the black hole in the form (see Narayan & Yi 1995b),

$$\begin{aligned} p &= 1.87\times10^{16}\alpha^{-1}m^{-1}\dot{m}r^{-5/2}\,\mathrm{gcm^{-1}s^{-2}}, \\ n_e &= 5.91\times10^{19}\alpha^{-1}m^{-1}\dot{m}r^{-3/2}\,\mathrm{cm^{-3}} \\ q^+ &= 2.24\times10^{20}m^{-2}\dot{m}r^{-4}\,\mathrm{ergscm^{-3}s^{-1}}, \\ c_\mathrm{s}^2 &= 1.67\times10^{20}r^{-1}\,\mathrm{cm^2\,s^{-2}}, \end{aligned} \tag{1}$$

where m, $\dot{m}$ and r are in units of solar mass, Eddington rate ($\dot{M}_\mathrm{Edd} = 1.39\times10^{18}m$ g/s), and Schwarzschild radius, respectively.

The ion number density is $n_i = n_e/1.077$, and the ion and electron temperatures closely follow

$$T_i + 1.077T_e = 1.98\times10^{12}r^{-1}\mathrm{K}. \tag{2}$$

The energy transfer from ions to electrons is given by Stepney (1983) and is approximated for the two-temperature advection-dominated hot flow (Liu et al. 2002) as

$$\begin{aligned} q_{ie} &= 3.59\times10^{-32}\mathrm{gcm^5s^{-3}deg^{-1}}\,n_en_iT_i\left(\frac{kT_e}{m_ec^2}\right)^{-3/2} \\ &= 1.05\times10^{35}T_e^{-3/2}\alpha^{-2}m^{-2}\dot{m}^2r^{-4}\,\mathrm{gcm^{-1}s^{-3}deg^{3/2}}. \end{aligned} \tag{3}$$

The coupling temperature is reached when viscous and compressive heating are balanced by the transfer of heat from the ions to the electrons, $q_{ie} = q^+ + q^c$, which yields

$$T_\mathrm{cpl} = 1.98\times10^9\alpha^{-4/3}\dot{m}^{2/3}. \tag{4}$$

The heat flux from the typical corona/ADAF to the radiating layer is derived from the energy balance in the corona, $\frac{dF_\mathrm{c}}{dz} = q_{ie}(T_e)$ assuming that the conductive flux is given by the expression $F_\mathrm{c} = -\kappa_0T_e^{5/2}dT_e/dz$ (Spitzer 1962) with $\kappa_0 = 10^{-6}\mathrm{erg\,s^{-1}cm^{-1}K^{-7/2}}$. (This value might be lower if e.g. chaotic magnetic fields reduce the effective conductivity). This

holds when the collisional mean free paths are small compared to the length over which the electron temperature changes. Solving for the conductive flux yields

$$F_{\rm c}^2(T_e) = (\kappa_0 K n_i n_e T_i)(T_{\rm em}^2 - T_e^2) \tag{5}$$

and at the coupling interface

$$F_{\rm c}^{\rm ADAF} \approx -(\kappa_0 K n_i n_e T_i)^{1/2} T_{\rm em}, \tag{6}$$

where "-" means a downward directed heat flow, $K = 1.64 \times 10^{-17} {\rm gcm^5 s^{-3} deg^{1/2}}$, $T_{\rm em}$ is the maximum electron temperature at height z_m corresponding to $F_c(z_m) = 0$ and can be derived by integration of $F_{\rm c} = -\kappa_0 T_e^{5/2} dT_e/dz$ from z_m to the interface by taking F_c in Eq.5, yielding

$$T_{\rm em} = 2.01 \times 10^{10} \alpha^{-2/5} \dot{m}^{2/5} r^{-2/5} {\rm K}. \tag{7}$$

The conductive flux from the corona arriving at the interface of the radiation region is then

$$F_{\rm c}^{\rm ADAF} = -6.52 \times 10^{24} \alpha^{-7/5} m^{-1} \dot{m}^{7/5} r^{-12/5}. \tag{8}$$

The energy balance in the radiating layer is determined by the incoming conductive flux, bremsstrahlung radiation flux, and the enthalpy flux carried by the mass evaporation/condensation flow,

$$\frac{d}{dz}\left[\dot{m}_z \frac{\gamma}{\gamma - 1}\frac{1}{\beta}\frac{\Re T}{\mu} + F_c\right] = -n_e n_i \Lambda(T). \tag{9}$$

This determines the evaporation/condensation rate per unit area, which is given by (Meyer et al. 2007)

$$\dot{m}_z = \frac{\gamma - 1}{\gamma}\beta \frac{-F_{\rm c}^{\rm ADAF}}{\frac{\Re T_i}{\mu_i}}\left(1 - \sqrt{C}\right) \tag{10}$$

with

$$C \equiv \kappa_0 b \left(\frac{0.25\beta^2 p_0^2}{k^2}\right)\left(\frac{T_{\rm cpl}}{F_c^{\rm ADAF}}\right)^2, \tag{11}$$

where $b = 10^{-26.56}\,{\rm g\,cm^5 s^{-3} deg^{-1/2}}$ (Sutherland & Dopita 1993), β corresponds to the ratio of gas pressure to total pressure, $p_0 = \frac{2}{\sqrt{\pi}} p$ the pressure in the radiating layer, $\gamma = \frac{8-3\beta}{6-3\beta}$ (Esin 1997), and $\mu_i = 1.23$ for an assumed chemical abundance of $X = 0.75$, $Y = 0.25$. Using Eqs.4 and 8 for $T_{\rm cpl}$ and $F_c^{\rm ADAF}$ and taking $\beta = 0.8$, we obtain

$$C = 0.96 \alpha^{-28/15} \dot{m}^{8/15} r^{-1/5}. \tag{12}$$

For $C < 1$, mass evaporates from the disk to the corona ($\dot{m}_z > 0$) since the conduction flux is not completely radiated away. On the other hand, for $C > 1$ coronal matter condenses into the disk ($\dot{m}_z < 0$) due to effective cooling by bremsstrahlung. The condition, $C = 1$,

separates the regions of evaporation and condensation and, hence determines, the outer radius of the inner disk, given as

$$\begin{aligned} r_{\rm d} &= 0.815\alpha^{-28/3}\dot{m}^{8/3} \\ &= 5864\left(\frac{\alpha}{0.2}\right)^{-28/3}\left(\frac{\dot{m}}{0.1}\right)^{8/3}. \end{aligned} \tag{13}$$

Thus, the determination of the condensation/evaporation region depends on mass accretion rate and viscosity parameter in the ADAF. The integrated condensation rate (in units of the Eddington rate) from $r_{\rm d}$ to any radius (r_i) of the disk is

$$\dot{m}_{\rm cnd} = \int_{R_i}^{R_d} \frac{4\pi R}{\dot{M}_{\rm Edd}}\dot{m}_z dR = 3.23\times10^{-3}\alpha^{-7}\dot{m}^3 f(r_{\rm i}/r_d),^{1} \tag{14}$$

with

$$f(x) = 1 - 6x^{1/2} + 5x^{3/5}. \tag{15}$$

The expressions for the size of the inner disk, r_d (eq.13) and the mass condensation rate, $\dot{m}_{\rm cnd}$ (eq. 14) reveal their sensitivity to the accretion rate and viscosity. Their dependence on the accretion rate ($\dot{m}$) for $\alpha = 0.2$ and $\alpha = 0.3$ are shown in Fig.3. It can be seen that an inner disk with size $r_d < 100$ only exists in a limited range of accretion rates, and this range strongly depends on α.

The radiation from the corona is dominated by bremsstrahlung in the radiating layer,

$$F_{\rm Brem} = \int_{z0}^{z1} n_e n_i \Lambda(T) dz,$$

where $z0$ and $z1$ are the lower and upper boundary of the radiating layer. By combining Eqs.9, 10 and 11, the flux is given by

$$F_{\rm Brem} = -F_c^{\rm ADAF}\sqrt{C} = 6.391\times10^{24}\alpha^{-7/3}m^{-1}\dot{m}^{5/3}r^{-5/2}\,{\rm erg\ s^{-1}\,cm^{-2}} \tag{16}$$

and the corresponding luminosity from the two sides of the disk corona is

$$\begin{aligned} \frac{L_{\rm Brem}}{L_{\rm Edd}} &= 2\int_{3R_S}^{R_d} 2\pi R F_{\rm Brem} dR = 0.0642\alpha^{-7/3}\dot{m}^{5/3}\left[1-\left(\frac{3}{r_d}\right)^{1/2}\right] \\ &= 0.0591\left(\frac{\alpha}{0.2}\right)^{-7/3}\left(\frac{\dot{m}}{0.1}\right)^{5/3}\left[1-\left(\frac{3}{r_d}\right)^{1/2}\right]. \end{aligned} \tag{17}$$

[1]Eq.(29) in Meyer et al. (2007) contains an error, without consequences in the paper since the formula was not further used. The true value is 3.23×10^{-3} as here

2.3. Compton Cooling-Dominant Corona

In the regime at relatively high mass accretion rates or with a luminous soft photon flux, the inverse Compton scattering process could be more effective for cooling the electrons than the vertical thermal conduction in an ADAF-like corona. The electron temperature in the upper coronal region then would be determined by Compton cooling. However, in the presence of an underlying cool disk conduction sets in at some height as the dominant cooling mechanism for the lower coronal layers. The additional Compton cooling within the corona leads to a relatively cool electron component in the corona/ADAF, resulting in a conductive flux from the corona to the radiating layer lower than that estimated in §2.2. The electron temperature in the corona is now determined by $q_{\rm ie} = q_{\rm cmp}$ where $q_{\rm cmp}$ is the Compton cooling rate given by

$$q_{\rm cmp} = \frac{4kT_e}{m_e c^2} n_e \sigma_T c u \tag{18}$$

where u is the soft photon energy density. By assuming that the soft photons for Compton scattering arise from the local underlying disk, u is expressed in terms of effective temperature in the local disk as $u(r) = \frac{1}{2} a T_{\rm eff}^4(r)$. The factor $\frac{1}{2}$ for the energy density of an isotropic blackbody photon field is taken since photons from the underlying disk cover only half of the sky of electrons in the corona. The effective temperature of a steady state disk with a constant mass accretion rate, given by $\sigma T_{\rm eff}^4 = \frac{3GM\dot{M}_{\rm d}}{8\pi R^3}\left[1 - \left(\frac{3R_S}{R}\right)^{1/2}\right]$, reaches at a maximum $T_{\rm eff,max}$ at $R = (49/36) \times 3R_S$ and is expressed as

$$T_{\rm eff}(r) = 2.05 T_{\rm eff,max} \left(\frac{3}{r}\right)^{3/4} \left[1 - \left(\frac{3}{r}\right)^{1/2}\right]^{1/4} \tag{19}$$

With this effective temperature for the soft photon field, the electron temperature of the corona is derived from Eq.18 as

$$T_{\rm ec} = 3.025 \times 10^9 \alpha^{-2/5} m^{-2/5} \dot{m}^{2/5} r^{1/5} \left[1 - \left(\frac{3}{r}\right)^{1/2}\right]^{-2/5} \left(\frac{T_{\rm eff,max}}{0.3keV}\right)^{-8/5} {\rm K}, \tag{20}$$

This temperature, $T_{\rm ec}$, is characteristic of the upper Compton cooling dominant corona and represents the maximum temperature within a given column at a distance, r. The conductive flux from the corona to the coupling interface is calculated from Eq.6 by replacing $T_{\rm em}$ with $T_{\rm ec}$ and is given by

$$F_c^{\rm ADAF} = -9.816 \times 10^{23} \alpha^{-7/5} m^{-7/5} \dot{m}^{7/5} r^{-9/5} \left[1 - \left(\frac{3}{r}\right)^{1/2}\right]^{-2/5} \left(\frac{T_{\rm eff,max}}{0.3keV}\right)^{-8/5} {\rm erg\,s^{-1}\,cm^{-2}}, \tag{21}$$

Since the Compton cooling rate is much lower than the bremsstrahlung rate in the radiating layer, the energy balance and, hence, the evaporation/condensation rate is the same as in the conduction dominant cooling case, except for the fact that the conductive flux expressed in Eq.10 is replaced by Eq.21. With this expression for the conductive flux, the critical condensation radius and the integrated condensation rate are derived by setting $C = 1$ (in Eq.11) and by integrating Eq.10 respectively, yielding

$$r_{\rm d}\left[1-\left(\frac{3}{r_d}\right)^{1/2}\right]^{-4/7} = 14.417\alpha^{-4/3}m^{4/7}\dot{m}^{8/21}\left(\frac{T_{\rm eff,max}}{0.3keV}\right)^{16/7}, \tag{22}$$

and

$$\dot{m}_{\rm cnd}(r) = A\left\{2B\left[\left(\frac{r_{\rm d}}{r}\right)^{1/2}-1\right]-\int_{r/3}^{r_{\rm d}/3}x^{1/5}\left(1-x^{-1/2}\right)^{-2/5}dx\right\} \tag{23}$$

where

$$A = 6.164\times10^{-3}\alpha^{-7/5}m^{-2/5}\dot{m}^{7/5}\left(\frac{T_{\rm eff,max}}{0.3keV}\right)^{-8/5} \tag{24}$$

and

$$B = 3.001\alpha^{-14/15}m^{2/5}\dot{m}^{4/15}\left(\frac{T_{\rm eff,max}}{0.3keV}\right)^{8/5}\left(\frac{r}{3}\right)^{1/2}. \tag{25}$$

There is either no solution or two solutions for r_d in Eq.22, depending on system parameters. In the case of no solution, mass does not condense into the disk by Compton cooling, but rather evaporates from the disk to the corona. The two solutions r_{d1} and r_{d2} determined by Eq.22 lie at both sides of the distance $r = (81/49)\times 3$, yielding a spatial extent for the condensation region described by $r_{d1} < r < r_{d2}$.

The total condensation rate to the inner disk is the integral from $r_{\rm d2}$ to $r_{\rm d1}$. Since the accretion rate in the disk increases with decreasing distance until $r = r_{d1}$, the disk effective temperature does not reach its maximum at $r_{\rm tmax} = (49/36)\times 3$, but at some distance slightly smaller than it (depending on the system parameters). However, the true maximal effective temperature is not much larger than the value at $r_{\rm tmax}$. In the following we assume the maximal effective temperature is reached at $r_{\rm tmax}$, which is a good approximation.

Thus, for a Compton cooling dominant corona, the region where matter condenses from the corona to the disk and the total condensation rate are determined by the mass of the black hole, the mass accretion rate, effective temperature of the soft photon radiation, and the disk viscosity parameter. Fig.4 shows that for given black hole mass, $m = 10$, and disk temperature, $T_{\rm eff,max} = 0.3keV$, the size of the inner disk and the condensation rate increase with accretion rate. For larger α values, both the size of the inner disk and the mass condensation rate decrease for a given m and $T_{\rm eff,max}$.

If the effective temperature is assumed to originate from disk accretion fed by condensation, the maximal effective temperature at $r_{\rm tmax}$ is no longer a free parameter,

$$\begin{aligned} T_{\rm eff,max} &= 1.3348\times10^7\,{\rm K}m^{-1/4}\dot{m}_{\rm cnd}^{1/4}(r_{\rm tmax}) \\ &= 0.2046{\rm keV}\left(\frac{m}{10}\right)^{-1/4}\left[\frac{\dot{m}_{\rm cnd}(r_{\rm tmax})}{0.01}\right]^{1/4}. \end{aligned} \quad (26)$$

Replacing $T_{\rm eff,max}$ in Eqs.22, 24 and 25, Eq.23 becomes a non-linear equation for $\dot{m}_{\rm cnd}(r_{\rm tmax})$ and can be numerically solved for given α, m and $\dot{m}$. The integrated condensation rate at any distance r can then also be calculated for a known $T_{\rm eff,max}$ using Eq.26.

Finally, the luminosity associated with the inverse Compton scattering process in the corona can be calculated as

$$L_{\rm cmp}=\int_{R_{\rm d1}}^{R_{\rm d2}}2\pi RH\frac{4kT_e}{m_ec^2}n_e\sigma_T 4\sigma T_{\rm eff}^4(R)dR. \quad (27)$$

Replacing the temperature T_e by Eq.20 and the density by Eq.1, we have

$$\frac{L_{\rm cmp}}{L_{\rm Edd}}=0.392\alpha^{-7/5}m^{3/5}\dot{m}^{7/5}\left(\frac{T_{\rm eff,max}}{0.3keV}\right)^{12/5}\int_{r_{\rm d1}/3}^{r_{\rm d2}/3}x^{-23/10}\left(1-x^{-1/2}\right)^{3/5}dx. \quad (28)$$

2.4. Compton Dominant or Conduction Dominant-Cooling?

In general, cooling from both the Compton scattering and thermal conduction processes should be included, however, in order to obtain analytical results we have only considered the cases when one of these processes is dominant. In the following we delineate the physical regime in which Compton cooling is important. One approach for determining the importance of Compton and conduction cooling in the corona is to compare the electron temperatures corresponding to the Compton cooling and conductive cooling regimes. The process resulting in a lower temperature is the more efficient cooling mechanism and thus would be dominant. As shown in previous work (e.g. Meyer et al. 2007), thermal conduction results in a vertical temperature distribution in the corona with the electron temperature decreasing from a maximum value $T_{\rm em}$ (see Eq.7) at the highest layer z_m to the coupling temperature $T_{\rm cpl}$ at the interface between the corona and radiating layer. On the other hand, for inverse Compton scattering, the electrons in the ADAF-like corona cool to a temperature $T_{\rm ec}$, which is independent of the vertical height. If, at any given height $z<z_m$, the electron temperature $T_e(z)$ determined by conduction is larger than the Compton cooling temperature $T_{\rm ec}$, Compton cooling should be more important. In this case, the maximum temperature $T_{\rm em}$ of Eq.7 is no longer relevant and the temperature from z to z_m is determined

by Compton cooling. That is, $T_e = T_{\rm ec}$, which becomes the maximum temperature in the upper coronal region. As long as the Compton temperature $T_{\rm ec}$ is less than the maximum temperature $T_{\rm em}$ as determined by conduction, Compton scattering should contribute to the coronal cooling. From $T_{\rm ec} \leq T_{\rm em}$, the critical radius where Compton cooling sets in is given by

$$r_{\rm cmp}\left[1-\left(\frac{3}{r_{\rm cmp}}\right)^{1/2}\right]^{-2/3} \leq 23.487 m^{2/3}\left(\frac{T_{\rm eff,max}}{0.3keV}\right)^{8/3}. \quad (29)$$

There exists a minimum at $r = (16/9)\times 3$ in the function for $r_{\rm cmp}$ on left-hand side of Eq.29. Thus, for this equation there is either no solution, implying that Compton cooling is unimportant or two solutions exist interior and exterior to $r = (16/9)\times 3$, which determines the Compton dominant region, $r_{\rm cmp1} < r < r_{\rm cmp2}$. This indicates that Compton cooling is non-negligible in the inner region ($r \sim 16/3$) for X-ray binaries if the disk effective temperature is not very low. For given M and $T_{\rm eff,max}$, say, $M = 10M_\odot$ and $T_{\rm eff,max} = 0.3$keV, the Compton dominant region $3.03 < r < 96$ follows, whereas for $M = 10M_\odot$ and $T_{\rm eff,max} = 0.2$keV, a smaller region $3.16 < r < 28.5$ follows. Fig.2 illustrates the radial extent where Compton cooling or conductive cooling is important in terms of the disk effective temperature in the innermost region for black hole masses of $m = 10$ and $m = 6$. It can be seen that, for typical X-ray binaries, the Compton cooling plays a role if the effective temperature in the inner disk is higher than about 0.14 keV.

2.5. Caveats

We wish to point out that the dependence of the ADAF solutions on the viscosity parameter α not only appears explicitly via its power-law dependence, as shown in Eq.1, but also implicitly through the coefficients of these solutions (Narayan & Yi 1995b). The values of the coefficients in Eq. 1 are derived by assuming $\alpha = 0.2$. As this dependence is weak, we neglect the implicit dependence in the following analysis when α is varied. Similarly, the coefficients in the ADAF solution also implicitly depend on the parameterized magnetic field β. In this work $\beta = 0.8$ is assumed based on results of the MHD simulation of Sharma et al. (2006). Compressive heating in the ADAF ($q^c = \frac{1}{1-\beta}q^+$) is also calculated for this value. As remarked earlier, the influence of the magnetic field on the vertical conduction is not discussed in our present analysis. Furthermore, the effects of irradiation and disk reflection are assumed to be unimportant since it is not expected to be significant for the small size of the weakly emitting inner disk that is characteristic for the low/hard state although it can lead to additional heating of the disk (see §5). Finally, we do not introduce a color correction factor to describe the spectral hardening factor of the disk in our simple model since such

a description is not an adequate description of the spectrum at the low mass accretion rate levels (see Shimura & Takahara 1995) in the inner disk of our systems in their low hard state.

3. Results

For a system with mass accretion rates lower than the maximum evaporation rate, corresponding to the hard-soft state transition, a gap forms in the disk by the efficient evaporation of matter at about a few hundred Schwarzschild radii. An inner cool remnant disk can be present extending from the ISCO to the critical condensation radius $r_{\rm d}$. This inner disk is fed by the condensing matter from its overlying corona and the accretion rate in the cool disk represents the integrated condensation rate. The coexistence of this inner cool disk and a coronal gap can yield an intermediate state spectrum characterized by both hard and soft components. Here, the strength of the soft component depends on the condensation rate and the inner disk size, both of which are determined by the system parameters, i.e. the mass of the black hole, the mass accretion rate, and the viscosity parameter.

3.1. Illustrative Examples for Conduction Dominant Cooling

For a typical X-ray binary with $M = 10M_{\odot}$ and standard disk viscosity parameter, $\alpha = 0.2$, the accretion rate should be less than the corresponding transition rate, 0.02, if the system is in the low or intermediate state. As an example, we adopt a value for the mass accretion rate of $\dot{m} = 0.01$. Based on the analysis presented in Sect.2.2 for the conduction dominant cooling model, a critical condensation radius of $r_d = 12.6$, a total condensation rate of $\dot{m}_{\rm cnd} = 4.70 \times 10^{-5}$, an inner disk effective temperature of $T_{\rm eff,max}$ =0.05keV, and a luminosity of $L/L_{\rm Edd} = 6.53 \times 10^{-4}$ are found. To check the consistency of the solution, the critical radius for the Compton cooling region was calculated. A Compton dominant cooling region was not found to exist, implying that the conduction dominant model is consistent. For lower mass accretion rates, $\dot{m} < 0.01$ or larger coronal viscosity parameters, $\alpha > 0.2$, both the disk size and the mass condensation rate rapidly decrease. Although the conductive cooling model remains a valid description, the inner disk vanishes for $\dot{m} < 0.006$ (for $\alpha = 0.2$) or $\alpha > 0.233$ (for $\dot{m} = 0.01$). For higher mass accretion rates ($\dot{m} > 0.01$) or smaller viscosity parameters, the condensation radius and mass condensation rate increase, leading to higher disk temperatures. Only for sufficiently high mass accretion rates (e.g. $\dot{m} = 0.03$ but standard viscosity, $\alpha = 0.2$), or sufficiently small viscosities (e.g. $\alpha = 0.14$, but unchanged accretion rate, $\dot{m} = 0.01$), must Compton cooling be taken into account in describing the physical state of the inner region.

3.2. Illustrative Examples for Compton Dominant Cooling

To illustrate an X-ray binary where Compton cooling plays an important role, we consider a system with a black hole mass of $M = 10M_{\odot}$ and a viscosity parameter $\alpha = 0.35$, but assume a higher mass accretion rate $\dot{m} = 0.11$. As discussed in §3.1, Compton cooling is expected to be an important cooling process in the inner region. Calculations based on conduction alone would yield condensation from the ISCO up to $r = 41$, resulting in a condensation rate of 2.79×10^{-3} times the Eddington rate. This leads to a maximal effective temperature of the inner disk of 0.14 keV (Eq.26). At such a temperature, Compton cooling becomes important from $r = 4$ until $r = 8$ (as calculated from Eq.29).

Therefore, in the case of $\alpha = 0.35$ and $\dot{m} = 0.11$, cooling in the corona is dominated by the Compton scattering in the inner region and the vertical conduction in the surrounding region. By presuming a value for the disk effective temperature, we calculate the condensation rate from Eqs.22-25 and derive the effective temperature from Eq.26. If this temperature matches the presumed value, the solution for the condensation rate is self-consistent. By iteration we find a consistent solution for the total condensation rate, $\dot{m}_{\rm cnd} = 3.0 \times 10^{-3}$, obtained by integration from an inner Compton dominant region ($3.7 < r < 10.6$) and an outer conduction dominant region ($10.6 < r < 41$), with a disk effective temperature $T_{\rm eff,max}$=0.15keV at $r_{\rm tmax}$.

In the above example, Compton cooling is not very strong, leading to a slight increase in the rate of condensation. For very efficient Compton cooling, the decrease in the conductive flux results in a significant increase in the condensation rate. To illustrate such a case we assume $\alpha = 0.4$, $\dot{m} = 0.16$, and $m = 10$. For this set of parameters, calculations based on the Compton cooling model show that the coronal gas condenses into the disk from $r = 30.5$ to $r = 3.08$, resulting in a mass condensation rate of $\dot{m}_{\rm cnd} = 0.01$. Such a rate leads to a consistent effective temperature of $T_{\rm eff,max} = 0.205$keV at $r_{\rm tmax}$. On the other hand, calculation based on the conduction model shows a condensation rate of only 0.003, much smaller than predicted by Compton cooling. Further calculations of the Compton dominant region show that the Compton scattering dominates the coronal cooling nearly throughout the condensation-fed inner disk.

Examples for various values of the viscosity and accretion rate are listed in Table 1. It is shown that the conduction cooling leads to low condensation rates and hence low disk temperatures, while the Compton cooling results in high condensation rates and hence high effective temperatures. For comparable viscosity values, the Compton cooling becomes efficient at high accretion rates.

Neglecting the upper limit to the accretion rates, we show in Fig.5 the dependence of the

condensation rate on the mass accretion rate for the case of Compton dominant cooling in the inner corona and conduction dominant cooling in the outer corona. Condensation caused by conduction alone is also shown for comparison. It can be seen that the condensation is strong for Compton cooling, though it only dominates over conduction in the inner region.

4. Comparison with Observations

To make a meaningful comparison between observations and theory it is important to recognize that the observations provide information on the luminosity rather than the mass accretion rate. In the case of an optically thick standard thin disk, the mass accretion rate is deduced from the luminosity, $\dot{M} = L/\eta c^2$ by assuming an energy conversion efficiency of $\eta = 0.1$. However, in an ADAF-like corona, η is less than 0.1 and its variation depends on the structural disk parameters (p, T_e, etc), and therefore is implicitly determined by α, m, and $\dot{m}$. For a Compton cooling dominant corona the main contribution to the luminosity is due to inverse Compton scattering. Bremsstrahlung radiation from the radiation layer could also contribute, but as a small part. Therefore, with observationally inferred mass and effective temperature, a value for viscosity, and a tentative $\dot{m}$, we calculate numerically the radiative luminosity from both Compton scattering (Eq.28) and Bremsstrahlung (Eq.17) . If the derived luminosity is not equal to the observed value, the accretion rate is varied and the calculation repeated until a consistent luminosity is obtained. In this way, the accretion rate can be found. The crucial issue in the modeling is whether a value for $\dot{m}$ exists which predicts condensation rather than evaporation.

In the case of a corona dominated by thermal conduction, the luminosity is due to bremsstrahlung radiation, and the mass accretion rate only depends on the observed luminosity and the assumed α in the form

$$\dot{m} = 5.196\alpha^{7/5} \left(\frac{L_{\rm Brem}}{L_{\rm Edd}}\right)^{3/5} \left[1 - \left(\frac{3}{r_d}\right)^{1/2}\right]^{-3/5}, \tag{30}$$

where the the factor $\left[1 - \left(\frac{3}{r_d}\right)^{1/2}\right]^{-3/5}$ is approximately unity as long as r_d is not very small. The inner disk size r_d, the condensation rate, and the effective temperature are thus determined from Eq.13, Eq.14 and Eq.26 respectively. We note that the conduction model is based on the assumption that Compton cooling is negligible and would only be consistent with the observations for condensation rates yielding low disk temperatures (from Eq.26).

A constraint on the viscosity parameter can be obtained from the mass accretion rate corresponding to the transition between spectral states. As shown in previous work by Meyer

et al. (2000a), the maximum evaporation rate, representing the hard-soft transition rate, roughly depends on the value of the viscosity parameter as $\dot{m}_{\rm tr} \propto \alpha^3$. In the intermediate state discussed here, the mass accretion rate cannot be larger than this transition rate for, otherwise, the optically thick disk extends to the ISCO without a coronal gap, resulting in a soft thermal dominated spectrum.

4.1. GX339-4

Based on the optical spectroscopy of GX339-4 during outburst, Hynes et al. (2003) infer an orbital period of 1.7557 days and a mass function of 5.8 $M_\odot$ for the system. For a likely distance we take 8 kpc and for the black hole mass 10 $M_\odot$ (see Zdziarski et al. 2004). Recently, Miller et al. (2006b) observed GX 339-4 during the low hard state with XMM Newton and found a soft component of $kT = 0.3$keV, interpreting it to arise from an inner disk extending to the ISCO. Such a weak disk near the black hole is very difficult to explain within the framework of standard accretion disk models. As the density of the reflecting medium inferred from observations is low (Miller et al. 2006b), the inner disk must be spatially limited in extent. At these low temperatures, in contrast to the 1-2keV spectrum in the soft state, a small inner disk would also be necessary in order that strong irradiation by the corona can be avoided. Given an unabsorbed flux of 5.33×10^{-9}ergs s^{-1}cm^{-2} (Miller et al. 2006b), the luminosity is $L/L_{\rm Edd} = 0.03$. At this luminosity and the characteristic power-law spectrum of GX 339-4 in the low hard state, Compton scattering could be dominant. Upon comparing the electron temperature obtained from analysis for the two cooling mechanisms, we confirm that Compton cooling is important from the innermost region $r = 3.03$ up to $r_{\rm cmp} = 95.7$ (by Eq.29). Even if a colour correction of 1.7 (Shimura & Takahara 1995) is assumed, the Compton cooling is still dominant in the inner region to the distance of $r = 18$. Hence, we consider GX 339-4 in terms of the Compton dominant condensation model.

With the black hole mass, luminosity, and effective temperature taken from the observations, and a standard value 0.2 for α, it is found that the accretion rate is $\dot{m} = 0.024$. This yields an inner disk extending to a distance of 99.5 Schwarzschild and a luminosity ratio of 21.8% between the disk and the corona. Adopting a larger viscous value, $\alpha = 0.3$, one obtains an accretion rate of 0.037. The disk size is $r_{\rm d} = 66.5$ and disk luminosity fraction is 12.7%, smaller than the case of standard viscosity value. A further increase in the viscosity to $\alpha = 0.4$ leads to a smaller inner disk and a lower disk luminosity fraction. Detailed fitting results are presented in Table 2, where for a given value of α, a value for $\dot{m}$ is found, which leads to a luminosity consistent with the inferred value. The corresponding spatial extent of the condensation region, the condensation rate, the effective temperature, as well as the

ratio of the disk to corona luminosities are also listed.

By comparing modeling results, we find that a larger viscosity predicts a smaller disk size and disk contribution to the luminosity. We note that the condensation rate yields an effective temperature (as shown in column 7 in Table 2), which is lower than observed. This may indicate a need for an additional energy source above that associated with the accretion of condensed gas. For example, other processes, such as irradiation, may lead to additional heating of the gas in the disk surface. Notwithstanding the uncertainties in observationally determining the color temperature of the soft thermal component, the lack of agreement may also imply a need for a color correction factor, although, in that case, Compton cooling may not be as effective.

4.2. J1753.5-0127

We also can compare our model with the recent observations of J1753.5-0127 (Miller et al. 2006a), however there are significant uncertainties in the distance and mass of the black hole. Our comparisons, thus, should be only considered to be indicative and accurate modeling must await determinations of these parameters. XMM Newton observations of J 1753.5-0127 reveal a X-ray luminosity of $L_X/L_{\rm Edd} = 0.003(D/8.5kpc)^2(M/10M_\odot)$ in the range 0.5keV to 10keV and a hard X-ray spectral index of ~ 0.66 (Miller et al. 2006a). Extrapolating the luminosity to 100-200keV yields $\frac{L}{L_{\rm Edd}} \approx 0.01(D/8.5kpc)^2(M/10M_\odot)$. The fit to the X-ray spectrum reveals a cool disk component of $kT = 0.2$keV (Miller et al. 2006a). Taking $D = 8.5kpc$ and $M = 10M_\odot$, the Compton process would be dominant in the inner region from $r = 3.16$ to $r = 28.5$ as estimated from Eq.29. Therefore, to model this object, Compton cooling should be taken into account. For the standard viscosity, $\alpha = 0.2$, we find a mass accretion rate of $\dot{m} = 0.02$ would suffice to produce the luminosity from both Bremsstrahlung in the radiating layer and Compton scattering in the typical coronal region. The size of the inner disk is $r_{\rm d} = 33.4$ (from Eq.22), while from Eq.13 $r_{\rm d} = 80$. This implies that condensation begins at $r = 80$ due to conduction, while Compton cooling sets in at $r_{\rm d} = 28.5$ and dominates to $r_{\rm d} = 3.16$. In this case, the condensation rate is obtained from an integration from the outer conduction dominant region ($28.5 \leq r \leq 80$) to the inner Compton dominant region ($3.16 \leq r \leq 28.5$), yielding $\dot{m}_{\rm cnd} = 1.95 \times 10^{-3}$. The disk component contributes a relative large fraction (0.16) to the total luminosity.

A fit to J1753.5-0127 with larger viscosities has also been carried out, and the relevant results are listed in Table 2. The calculations show that at a fixed effective temperature, for larger viscosities the conduction cooling to the corona is less efficient and hence the Compton cooling becomes more important. Specifically, the inner disk becomes smaller,

the condensation rate decreases, and disk becomes weaker relative to the corona. Future measurements of the disk luminosity fraction and the reflection component will provide further constraints on the viscosity.

5. Discussion and implications

The evaporation/condensation picture for the accretion geometry of black hole X-ray transient systems has been investigated to determine its applicability to the weak soft thermal component observed in the low hard states of GX339-4 and J1753.5-0127. The model for the mass and energy exchange between the corona and an underlying disk developed earlier, based on the thermal conduction of energy, has been extended to include the effects of coronal cooling associated with the inverse Compton scattering process of soft X-ray photons. The numerical solutions for the disk structure reveal that the Compton dominated cooling region is more important for higher soft photon fluxes at all radii, with the radial extent $r_{\rm cmp}$ of the region independent of the mass of the accreting black hole component in the system. In addition, it is found that cool inner disks, contributing a small fraction of the total X-ray luminosity ($< 20\%$), can exist in the low hard state of black hole transient systems GX 339-4 and J1753.5-0127.

The fits to GX 339-4 and Swift J1753.5-0127 reveal that the theoretical disk temperatures are lower than the observationally inferred values, indicating that additional heating of the disk is required. We suggest that this heating is associated with coronal irradiation.

Specifically, for a corona in the form of a slab lying above the disk, nearly half of the total coronal emission impinges on the optically thick disk and is reprocessed as blackbody radiation (Haardt & Maraschi 1991; Liu et al. 2003). The luminosity associated with the irradiation is close to the observed luminosity. For GX 339-4, this irradiating luminosity is about 0.03 times the Eddington value. Its corresponding heating is equivalent to viscous dissipation in the disk with an additional accretion rate of 0.03 of the Eddington value, producing an effective temperature of about 0.27keV (from Eq.26). Taking into account the viscous dissipation from the accretion of condensing matter, the inner disk temperature can be similar to the observationally inferred value of 0.3keV. Similarly, for Swift J1753.5-0127, $L/L_{\rm edd} = 0.01$, and the disk is heated by irradiation to about 0.2keV, again, comparable to that observed.

The inclusion of irradiation does not affect the fits described in §4 since the disk temperature is fixed to the observed value. Although the effective temperature established by viscous dissipation is lower than 0.3keV, the additional heating from irradiation can lead to

improved comparisons between the theoretically derived and observed temperatures.

5.1. Range of luminosity over which cool inner disks exist

In the low hard state the luminosity range over which cool inner disks exist depends on whether condensation can occur. To determine the lower limit to the range we make use of the fact that the critical condensation radius should fulfill the condition that $r_d > 3$. In the case that conduction cooling dominates in the corona, this condition requires

$$\dot{m} > 1.63\alpha^{7/2}. \tag{31}$$

For a fixed viscosity parameter, $\alpha = 0.2$, a lower limit to the accretion rate for an inner disk to exist is $\dot{m} = 0.006$. The corresponding luminosity in this critical case is from a pure ADAF luminosity (rather than Bremsstrahlung), which could be as small as $\frac{L}{L_{\rm Edd}} = 0.001$, depending on the radiative efficiency of the ADAF accretion. At an accretion rate slightly higher than the critical value, the disk component, as measured by the disk size or by the disk luminosity fraction for example, could be very weak and hence Compton cooling is negligible. We note that this lower critical mass accretion rate is very sensitive to α.

For cases in which Compton cooling dominates in the corona, the lower limits to the accretion rate for condensation to a disk are greater than that given by the conduction model for $0.1 < \alpha < 0.4$. In particular, the lower limit to the accretion rate is 0.0245 (0.07) and to the luminosity is 0.008 (0.016) for $\alpha = 0.2(0.3)$.

Thus, the lower limit on the mass accretion rate or luminosity leading to the formation of an inner disk is set by the conduction model, which is found to depend on the viscosity parameter. For a $10M_\odot$ black hole, condensation could occur at an accretion rate as low as $\dot{m} = 0.006$ for a standard viscosity parameter $\alpha = 0.2$. However, if observations suggest high-temperature soft component (say, $T_{\rm eff} = 0.14$keV), Compton scattering must play a role in cooling of the corona, and the lower limit to the accretion rate is higher, corresponding to about $0.01L_{\rm Edd}$, depending on the viscosity.

Hence, our considerations of the two cooling regimes suggest cool inner disks may be present for systems with X-ray luminosities as low as 0.001-0.01 $\rm L_{Edd}$. This is of particular interest for J1753.5-0127 since it remained in a hard state throughout its outburst, suggesting that a spectral transition from a hard state to a soft state during an outburst is not a necessary condition for the formation of an inner disk in the hard state. Observations of J1753.5-0127 at even lower luminosity levels would be especially valuable in constraining the model parameters further. Of particular interest, we note that the observations of different classes of systems suggest that the viscosity parameter is relatively high ($\alpha \sim 0.1 - 0.4$, see

King et al. 2007; exceeding more than 0.5 from MHD simulation by Sharma et al. 2006), overlapping with the range of values inferred from our modeling.

An upper bound on the luminosity for which an inner disk exists in the hard state can also be estimated. The luminosity given by the condensation model increases with increasing accretion rate and decreasing viscosity. Thus, the upper bound is constrained by the highest accretion rate and lowest viscosity. For example, at a transition accretion rate of 0.02 (0.0675), the upper bound to the luminosity is 0.003 (0.009) for $\alpha = 0.2(0.3)$. We point out that at the upper limit of $\dot{m} = 0.1$ suggested by Narayan et al. (1995b) for the existence of an ADAF, the lowest viscosity is 0.342. A lower value for α would correspond to a transition rate lower than 0.1 (from $\dot{m}_{\rm tr} \propto \alpha^3$), and the system would no longer lie in the low/hard state. Hence, in this limit, an upper bound on the luminosity is 0.02 for this transition accretion rate. This is in good agreement with a hard-to-soft transition luminosity of 1%-4% found in X-ray binaries (Maccarone 2003).

5.2. A mass-independent process

It has been shown in previous investigations of the energy and mass exchange between the accretion disk and its corona that the results of both the evaporation process, i.e., the Eddington scaled evaporation rate ($\dot{M}_{\rm evap}/\dot{M}_{Edd}$) and its distribution with respect to the scaled distance ($R/R_{\rm S}$) and the condensation process to a truncated inner cool disk are not dependent on the mass of the black hole (Liu et al. 2002; Liu et al. 2006; Meyer et al. 2007; see also Eqs.13 and 14). By including the effect of Compton cooling in the present study, the condensation rate appears to depend on the mass of the black hole and the disk effective temperature, as shown in Eqs.22 and 23. If the accretion of the condensing matter is the only energy source for establishing the thermal properties of the disk, the effective temperature is no longer a free parameter, but is determined by Eq.26. Replacing $T_{\rm eff,max}$ in Eqs. 22, 24, and 25 by Eq.26, we find that the critical radius where condensation takes place, r_d, and the quantities A and B only depend on the disk viscosity parameter and the mass accretion rate as given by

$$r_{\rm d}\left[1-\left(\frac{3}{r_d}\right)^{1/2}\right]^{-4/7} = 311.43\alpha^{-4/3}\dot{m}^{8/21}\dot{m}_{\rm cnd}^{4/7}, \tag{32}$$

$$A = 7.174\times10^{-4}\alpha^{-7/5}\dot{m}^{7/5}\dot{m}_{\rm cnd}^{-2/5}, \tag{33}$$

$$B = 25.785\alpha^{-14/15}\dot{m}^{4/15}\dot{m}_{\rm cnd}^{2/5}\left(\frac{r}{3}\right)^{1/2}. \tag{34}$$

With above expression for r_d, A and B we obtain from Eq.23 a non-linear equation describing the condensation rate $\dot{m}_{\rm cnd}(r)$, which depends on α and the Eddington scaled accretion rate $\dot{m}$, but independent of m. For any given accretion rate and viscosity parameter, the condensation rate is determined by Eq.23. Likewise, the extent of the Compton cooling dominant region, the electron temperature in the corona, and the Compton luminosity are determined as

$$r_{\rm cmp}\left[1-\left(\frac{3}{r_{\rm cmp}}\right)^{1/2}\right]^{-2/3} \leq 846.71\dot{m}_{\rm cnd}^{2/3}, \tag{35}$$

$$T_{\rm ec} = 3.52\times10^{8}{\rm K}\alpha^{-2/5}\dot{m}^{2/5}\dot{m}_{\rm cnd}^{-2/5}r^{1/5}\left[1-\left(\frac{3}{r}\right)^{1/2}\right]^{-2/5}, \tag{36}$$

$$\frac{L_{\rm cmp}}{L_{\rm Edd}} = 9.88\alpha^{-7/5}\dot{m}^{7/5}\dot{m}_{\rm cnd}^{3/5}\int_{r_{\rm d1}/3}^{r_{\rm d2}/3} x^{-23/10}\left(1-x^{-1/2}\right)^{3/5}dx. \tag{37}$$

Thus the condensation process and the thermal state of the corona (i.e., the electron temperature) are independent on the mass of the black hole. Taking into account the mass-independent features of the previously developed model and its extension in this study, we conclude that the simple description of the accretion process within the framework of an evaporation/condensation picture can be applied not only to stellar mass black holes in X-ray binary systems, but also to supermassive black holes in active galactic nuclei. The presence of a cool disk in the innermost regions surrounding a supermassive black hole in a low state would directly contribute to the ultraviolet and optical emission and possibly indirectly via reflected X-ray emission from a spatially extended inner disk. In addition, it would provide a natural site of cool material where neutral iron could be present for the production of Fe fluorescent line emission at 6.4 keV (e.g. Tanaka et al. 1995). A more detailed study of the properties of such a cool disk would be especially illuminating for interpretations of Fe line profiles based on general relativistic broadening, though at present it is difficult to observe such a line spectrum from low luminosity active galactic nuclei.

This work was supported, in part, by the Theoretical Institute for Advanced Research in Astrophysics (TIARA) operated under Academia Sinica and the National Science Council Excellence Projects program in Taiwan administered through grant number NSC 95-2752-M-007-006-PAE. B.F. Liu acknowledges the support by the National Natural Science Foundation of China (NSF-10533050) and the BaiRenJiHua program of the Chinese Academy of Sciences.

REFERENCES

Dullemond, C. P., & Spruit, H. C. 2005, A&A, 434, 415

Eardley, D. M., Lightman, A. P., & Shapiro, S. L. 1975, ApJ, 199, L153

Esin, A. A., 1997, ApJ, 482, 400

Esin, A. A., McClintock, J. E., & Narayan, R. 1997, ApJ, 489, 865

Haardt, F., & Maraschi, L., 1991, ApJ, 380, L51

Hynes, R.I., Steeghs, D., Casares, J., Charles, P.A., & O'Brien, K. 2003, ApJ, 583, L95

King, A. R., Pringle, J. E., & Livio, M. 2007, MNRAS, 376, 1740

Laurent, P., & Titarchuk, L 2007, ApJ, 656, 1056

Liu, B. F., Mineshige, S., & Ohsuga, K., 2003, ApJ, 587, 571

Liu, B. F., Yuan, W., Meyer, F., Meyer-Hofmeister, E., & Xie, G. Z. 1999, ApJ, 527, L17

Liu, B. F., Mineshige, S., & Meyer, F., Meyer-Hofmeister, E., & Kawaguchi, T. 2002, ApJ, 575, L117

Liu, B. F., Meyer, F., & Meyer-Hofmeister, E. 2006, A&A, 454, L9

Maccarone, T. J. 2003, A&A, 409, 697

Mayer, M. & Pringle, J. E., 2007, MNRAS, 376, 435

McClintock, J.E., & Remillard, R.A., 2006, In: Compact Stellar X-ray Sources, eds. W.H.G. Lewin, M. van der Klis, Cambridge Univ. Press

Meyer, F., Liu, B. F., & Meyer-Hofmeister, E. 2000a, A&A, 361, 175

Meyer, F., Liu, B. F., & Meyer-Hofmeister, E. 2000b, A&A, 354, L67

Meyer, F., Liu, B. F., & Meyer-Hofmeister, E. 2007, A&A, 463, 1

Meyer, F., & Meyer-Hofmeister, E. 1994, A&A, 288, 175

Miller, J. M., Homan, J., & Miniutti, G. 2006a, ApJ, 652, L113

Miller, J. M., Homan, J., Steeghs, D., Rupen, M., Hunstead, R. W., Wijnands, R., Charles, P. A., & Fabian, A. C. 2006b, ApJ, 653, 525

Narayan, R. 2005, Ap&SS, 300, 177

Narayan, R., Mahadevan, R., & Quataert, E. 1998, In: The Theory of Black Hole Accretion Discs, eds. M.A. Abramowicz et al., Cambridge Univ. Press, p. 48

Narayan, R., & Yi, I. 1994, ApJ, 428, L13

Narayan, R., & Yi, I. 1995a, ApJ, 444, 231

Narayan, R., & Yi, I. 1995b, ApJ, 452, 710

Narayan, R., & Yi. I. 1995c, ApJ, 477, 585

Palmer, D. M., Barthelmy, S. D., Cummings, J. R., Gehrels, N., Krimm, H. A., Markwardt, C. B., Sakamoto,T.,& Tueller, J. 2005, Astron. Tel. 546

Pozdnyakov, L. A., Sobel, I. M., & Syunyaev, R. A. 1983, Astroph. & Space Phys. Res., 2, 189

Remillard, R. A., & McClintock, J. E. 2006, ARA&A, 44, 49

Ròżańska, A., & Czerny, B. 2000a, MNRAS, 316, 473

Ròżańska, A., & Czerny, B. 2000b, A&A, 360, 1170

Shakura, N. I., & Sunyaev, R. A. 1973, A&A, 24, 337

Shapiro, S. L., Lightman, A. P., & Eardly, D. M. 1976, ApJ, 204, 187

Sharma, P., Hammet, W., Quataert, E. et al. 2006, ApJ, 637, 952

Shaviv, G., & Wehrse, R. 1986, A&A, 159, L5

Shimura, T., & Takahara, F. 1995, ApJ, 445, 780

Spitzer L., 1962, Physics of Fully Ionized Gases, 2nd edition, Interscience Publ., New York, London

Sunyaev, R. A., & Titarchuk, L. G. 1980, A&A, 86, 121

Sutherland, R.S. & Dopita, M.A. 1993,ApJS, 88, 253

Tanaka, Y., Nandra, K., Fabian, A. C. et al. 1995, Nature, 375, 659

Tanaka, Y., & Shibazaki, N. 1996, ARA&A, 34, 607

Yuan, F., 2003, ApJ, 594, L99

Zdziarski, A. A., Gierliński, M., Mikolajewska, J. et al. 2004, MNRAS, 351, 791

Table 1. The condensation features of disk corona accretion around a $10M_\odot$ black hole. For given values of viscosity (α) and accretion rate ($\dot{m}$), the inner disk size (r_d), the total condensation rate ($\dot{m}_{\rm cnd}$) and its corresponding maximal temperature ($T_{\rm eff,max}$) are listed. The luminosity ($L/L_{\rm Edd}$) from Bremsstrahlung and Compton scattering (if Compton cooling sets in) and the dominant cooling mechanism or Compton dominant region are also shown.

α	$\dot{m}$	r_d	$\dot{m}_{\rm cnd}$	$T_{\rm eff,max}$(keV)	$L/L_{\rm Edd}$	Cooling mechanism
0.2	0.01	12.6	4.70×10^{-5}	0.05	6.52×10^{-4}	Conduction
0.3	0.04	11.6	1.60×10^{-4}	0.07	2.45×10^{-3}	Conduction
0.4	0.08	5.0	3.32×10^{-5}	0.03	1.83×10^{-3}	Conduction
0.2	0.03*	237	5.24×10^{-3}	0.17	1.57×10^{-2}	$3.3 < r_{\rm cmp} < 18$
0.35	0.11	41	3.00×10^{-3}	0.15	2.80×10^{-2}	$3.7 < r_{\rm cmp} < 10.6$
0.4	0.16	30.5	0.01	0.20	0.069**	Compton

*This is shown as an example for Compton cooling with the standard value of α, but the accretion rate exceeds the transition rate.

**This luminosity is over-estimated by the increase of optical depth of the corona.

Table 2: The fitting results for GX 339-4 and J1753. For every given value of α, an accretion rate, $\dot{m}$, is found, which predicts a luminosity consistent with the observational inferred value. r_d, $\dot{m}_{\rm cnd}$, $L/L_{\rm Edd}$, $L_{\rm d}/L_{\rm c}$ and T(keV) are the model predictions for the disk size, condensation rate, luminosity, ratio of the disk and corona luminosities, and the maximal effective temperature caused by accretion.

α	$\dot{m}$	r_d	$\dot{m}_{\rm cnd}$	$L/L_{\rm Edd}$	$L_{\rm d}/L_{\rm c}$	T(keV)
GX 339-4: $L/L_{\rm Edd}=0.03$, $M=10M_\odot$, $T_{\rm eff,max}=0.3$keV						
0.2	0.024	3.01–99.5	6.66×10^{-3}	0.03	21.8%	0.185
0.3	0.037	3.02–66.5	3.78×10^{-3}	0.03	12.7%	0.160
0.4	0.051	3.03–50.0	2.54×10^{-3}	0.03	8.4%	0.145
J1753.5-0127: $L/L_{\rm Edd}=0.01$, $M=10M_\odot$, $T_{\rm eff,max}=0.2$keV						
0.2	0.02	3.07–33.4	1.95×10^{-3}	0.01	18.9%	0.136
0.3	0.034	3.12–22.5	9.91×10^{-4}	0.01	9.6%	0.115
0.4	0.049	3.2–16.7	5.73×10^{-4}	0.01	5.7%	0.100

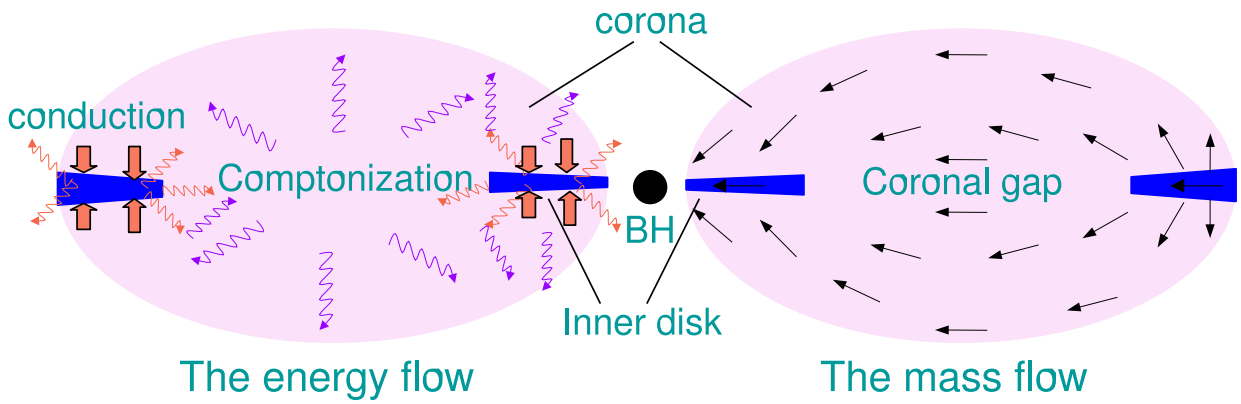

Fig. 1.— Schematic picture of the truncated outer disk separated from the inner disk by a coronal gap, indicating the energy and mass flow in the configuration.

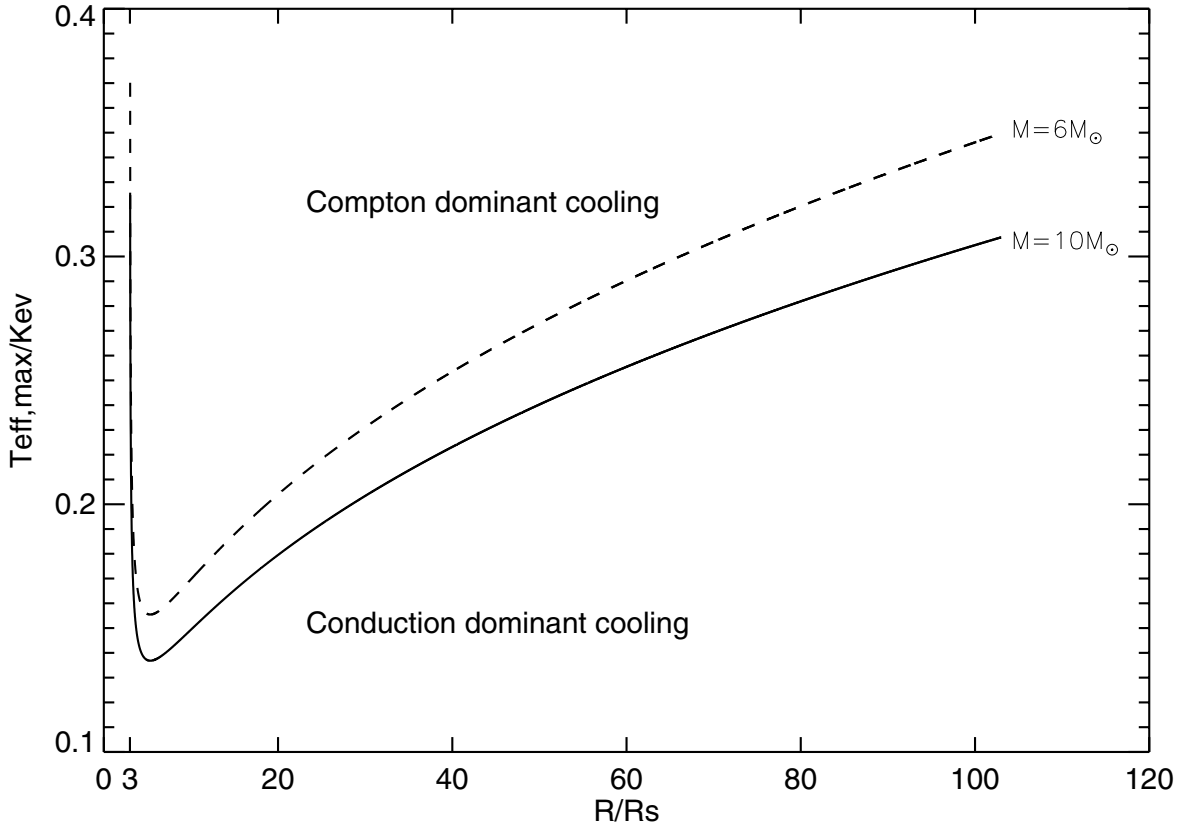

Fig. 2.— The radial region where Compton or conduction cooling dominates as a function of the innermost disk temperature. The curves represent the critical effective temperature of the inner disk, above which Compton cooling should be taken into account and below which the conduction dominant model is valid. The solid and dash lines correspond to a black hole mass of $m = 10$ and $m = 6$ respectively.

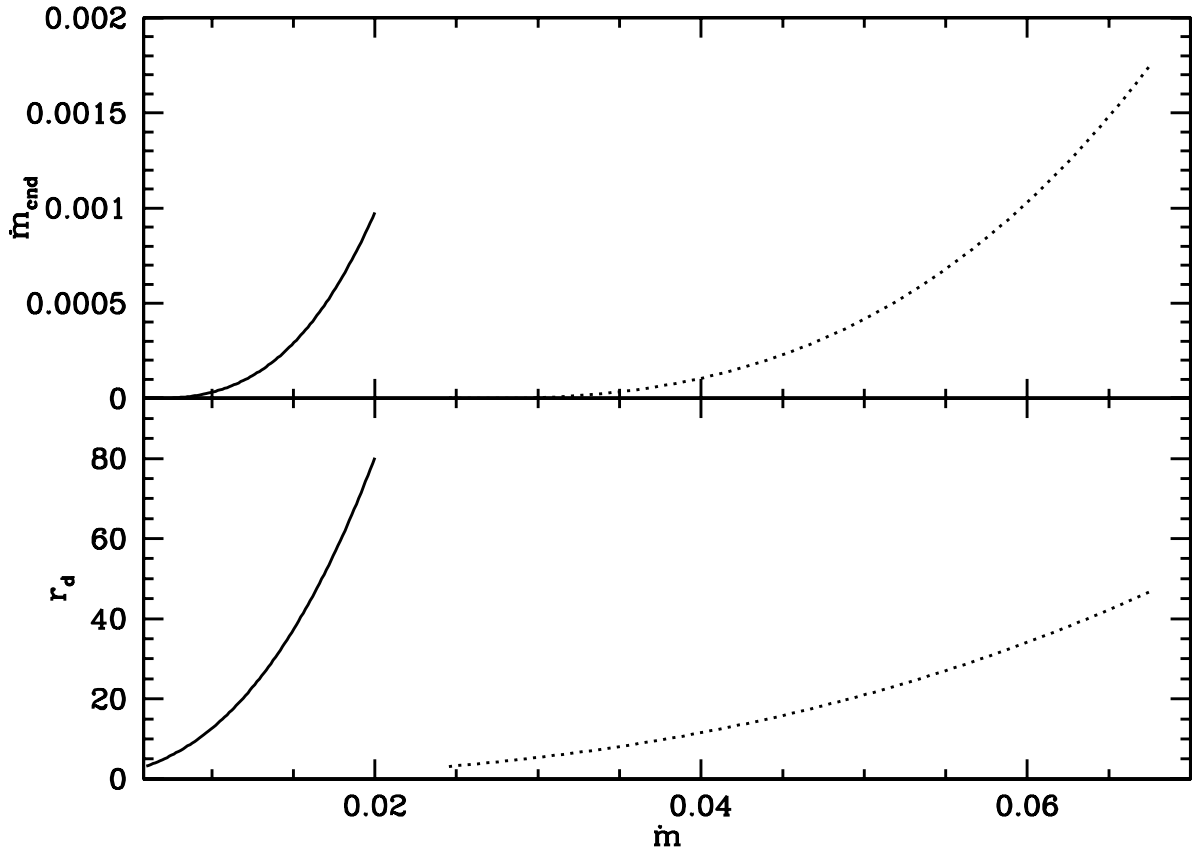

Fig. 3.— The dependence of the critical condensation radius (r_d) and the condensation rate ($\dot{m}_{\rm cnd}$, integrated from r_d to $r_{\rm tmax}$) on the accretion rate ($\dot{m}$) for a conductive cooling-dominant corona. The mass of black hole is fixed to $10M_\odot$. The values of the viscosity are $\alpha = 0.2$ (solid curves) and $\alpha = 0.3$ (dotted curves), respectively.

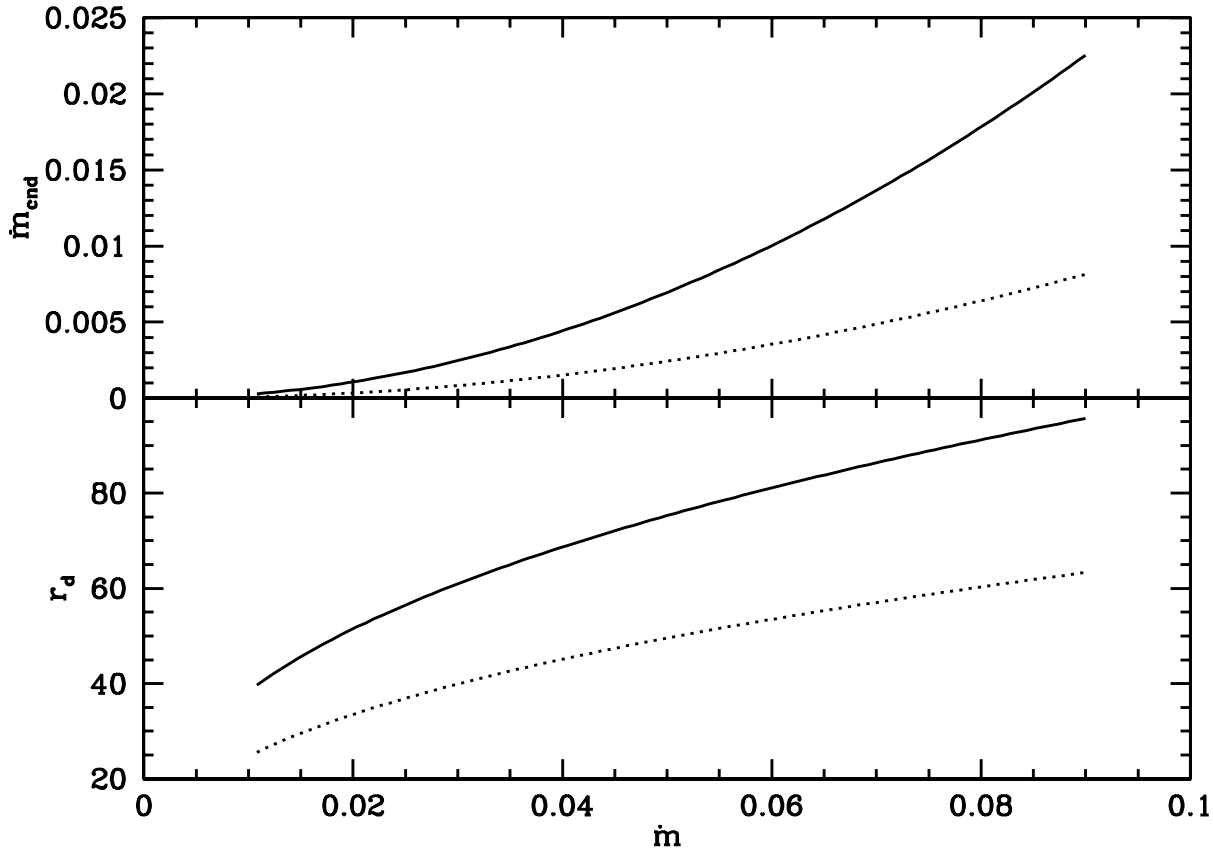

Fig. 4.— The dependence of the critical condensation radius (r_d) and the condensation rate ($\dot{m}_{\rm cnd}$, integrated from r_d to $r_{\rm tmax}$) on the accretion rate ($\dot{m}$) for a Compton cooling-dominant corona. The mass of black hole is fixed to $10M_\odot$ and the effective temperature of the disk $T_{\rm eff,max} = 0.3$keV. The values of the viscosity are $\alpha = 0.3$ (solid curves) and $\alpha = 0.4$ (dotted curves), respectively.

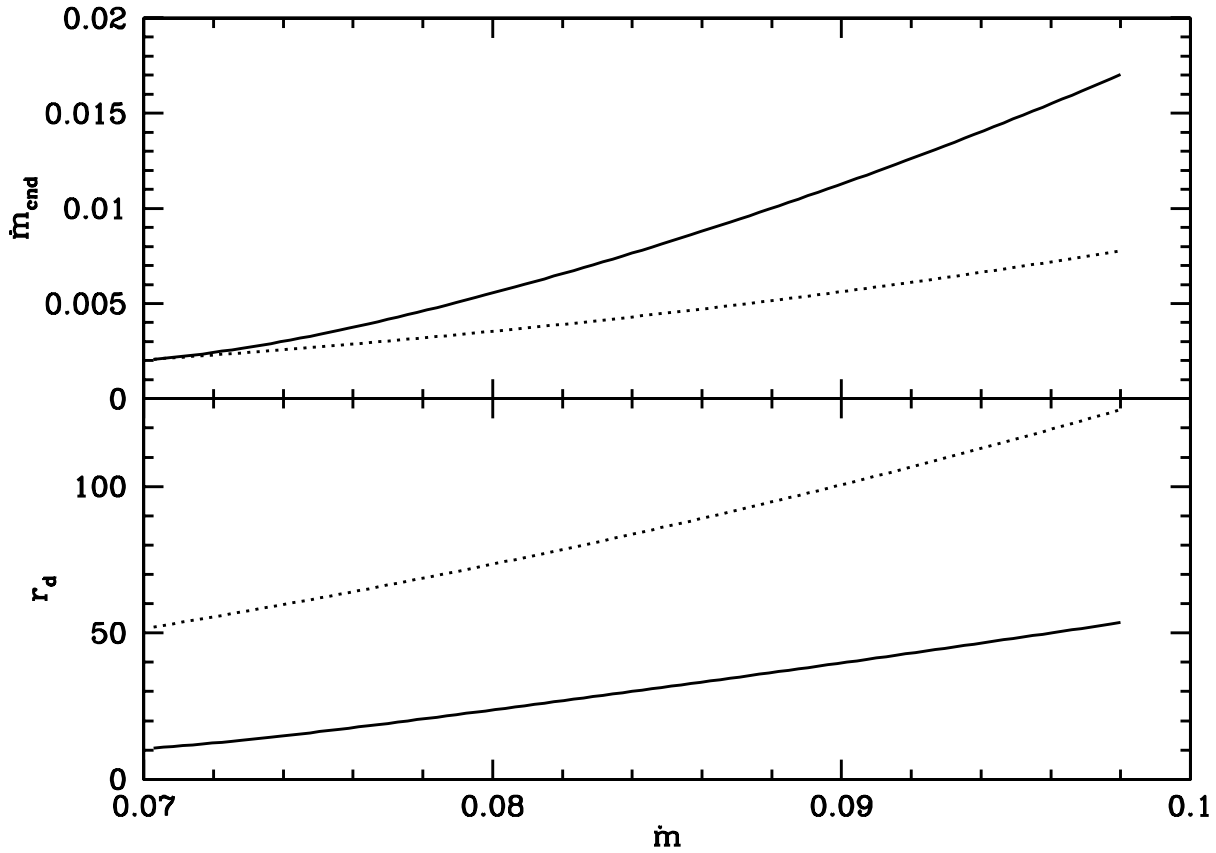

Fig. 5.— Comparison of the critical condensation radius (r_d) and the integrated condensation rate ($\dot{m}_{\rm cnd}$) for a conductive cooling and Compton cooling-dominant corona. The mass of black hole is fixed to $10M_\odot$, and the value of the viscosity is 0.3. The dotted curves refer to a conductive cooling corona as shown in Fig.3. The solid curves are for a Compton cooling dominant corona, where $\dot{m}_{\rm cnd}$ is integrated from an inner Compton dominant to an outer conductive dominant region. The smaller critical radius resulting from Compton cooling reflects the fact that Compton scattering is important mainly in the inner region. The higher condensation rate in the case of including Compton scattering also indicates that the Compton cooling can play an important role in condensation.